Association of Metallurgical Engineers of Serbia *Scientific paper*
AMES *UDC: 669.14-462*

FREE VIBRATION ANALYSIS OF FUNCTIONALLY GRADED NANOCOMPOSITE CYLINDRICAL PANEL REINFORCED BY CARBON NANOTUBE

J. E. Jam [1], A. Pourasghar [2], S. Kamarian [2], Nader Namdaran [1,*]

[1] *Composite Material & Technology Center, Tehran, Iran*
[2] *Mechanical Engineering Department, Razi University, Kermanshah, Iran*

Received 11.05.2013
Accepted 04.06.2013

Abstract

In this study, based on the three-dimensional theory of elasticity, free vibration characteristics of nanocomposite cylindrical panels reinforced by single-walled carbon nanotubes are considered. The carbon nanotube reinforced (CNTRC) cylindrical panels have smooth variation of carbon nanotube (CNT) fraction in the radial direction and the material properties are estimated by the extended rule of mixture. Suitable displacement functions that identically satisfy the boundary conditions at the simply supported edges are used to reduce the equilibrium equations to a set of coupled ordinary differential equations with variable coefficients, which can be solved by a generalized differential quadrature (GDQ) method. The results show that the kind of distribution and volume fraction of CNT have a significant effect on the normalized natural frequency.
Keywords: free vibrations, functionally graded materials (FGMs), nanocomposite, three-dimensional elasticity solution, cylindrical panel.

Introduction

The biggest specification of carbon nanotubes, which distinguishes them from the rest of the materials, is the abnormal mechanical, thermal, and electrical properties, and even more importantly their extraordinary property of fracture strength [1-5]. Also, all the data gathered from the experiments and simulations indicate that the direction of the nanotubes embedded in the matrix plays an important role in the determination of the mechanical properties of the reinforced material [6-8]. Fidelus *et al*. [9] investigated the thermo-mechanical properties of the nanocomposite, based on low volume fraction and random orientation of the single-walled carbon nanotubes. Han *et al*. [10] simulated the mechanical properties of polymer/carbon nanotube composites, using the molecular dynamics method and also investigated the effect of volume fraction of carbon

* Corresponding author: Nader Namdaran, nader_namdaran@yahoo.com

nanotubes on the mechanical properties of the nanocomposite. As it is stated in many of the researches performed, functionally graded materials (FGMs) are materials whose properties vary continuously through the thickness direction from one surface to the other one. Using the concept of FGMs, Shen [11, 12] showed that the functionally graded distribution of nanotube in the matrix improves the material properties. In these studies, the investigation of the non-linear bending of a functionally graded plate reinforced by carbon nanotubes under uniform and sinusoidal loading in a thermal environment was performed, and further the buckling of a cylindrical shell reinforced with carbon nanotubes was carried out under axial compressive loading in a thermal environment, and it was shown that the linear functionally grading of the material, increases the buckling load. Sobhani *et al*. [13] presented a three dimensional elasticity solution for the free vibration of a functionally graded cylindrical panel, and showed their results for a functionally grad cylindrical panel with random volume fraction and fiber angles along the thickness direction. Static and free vibration analyses of functionally graded structures have been investigated in many papers [14- 21]. The solution presented in the current paper is based on the numerical method of generalized differential quadrature, which leads to an eigenvalue problem. The convergence speed of this method is very high and some sample points are enough to reach an answer with a reasonably high accuracy. Tornabene *et al*. [14] also used the differential quadrature method for the free vibration analysis of a parabolic shell. In this paper, the free vibrations of a functionally graded cylindrical panel reinforced by carbon nanotubes are investigated, using the differential quadrature method. The material properties vary through the thickness direction, and are estimated by the micromechanical model. Since the micromechanical equations cannot distinguish the difference between the nano and micro scales, as a result in order to solve this problem, the effectiveness coefficient of (η) has been introduced, which is obtained from the compatibility of the results achieved from the extended rule of mixture, with the results achieved from the molecular dynamics method. The parametric study of the recent study is performed so as to show the effect of different distribution kinds of carbon nanotubes, including both symmetric and non-symmetric geometries, volume fraction of the nanotube, and different geometrical parameters on the free vibrations of the functionally graded cylindrical panel.

Problem Discussion

Consider the cylindrical panel shown in figure 1, with a finite length in the cylindrical coordinate system of r, θ, z, where r, θ, and z define the radial, circumferential, and axial directions, respectively. Properties of the material are a function of the radial coordinate the panel, in a way that the variations of the volume fraction of the nanotubes in the panel, happen to vary in four fashions as below, according to figure 2:

For kind V
$$V_{cn} = 2\left(\frac{r - r_i}{h}\right) V_{cn}^{*} \tag{1-a}$$

For kind Λ
$$V_{cn} = 2\left(\frac{r_o - r}{h}\right) V_{cn}^{*} \tag{1-b}$$

For kind X $$V_{cn} = 4\left|\frac{R-r}{H}\right|V_{cn}^{*} \quad (1\text{- c})$$

Where in the above relations, V_{CN} indicates the distribution kind of the carbon nanotubes in the cylindrical panel. Also, it is necessary to mention that for the uniform distribution in the panel, one must have $V_{cn} = V_{cn}^{*}$, where:

$$R = \left(\frac{r_i + r_o}{2}\right) \qquad V_{cn}^{*} = \frac{\rho^{m}}{\rho^{m} + \rho^{cn}(w^{cn})^{-1} - \rho^{cn}} \quad (2)$$

Wherein, w^{CN} is the weight percentage of the carbon nanotube, and ρ^{m} , ρ^{CN} are the density of the polymeric matrix and carbon nanotube, respectively.

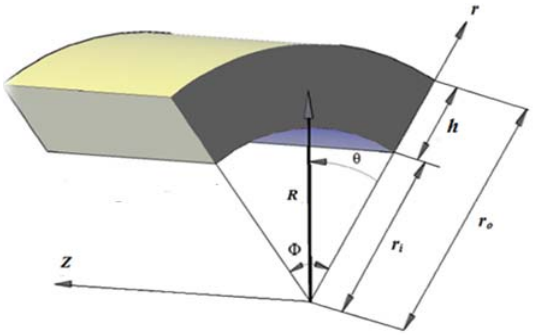

Fig. 1. Geometry of the cylindrical panel.

According to the generalized rule of mixtures, the effective Young's modulus and the effective shear modus are defined as follows [11]:

$$E_{11} = \eta_1 V_{cn} E_{11}^{cn} + V_m E^{m} \quad (3)$$

$$\frac{\eta_2}{E_{22}} = \frac{V_{cn}}{E_{22}^{cn}} + \frac{V_m}{E^{m}} \quad (4)$$

$$\frac{\eta_3}{G_{12}} = \frac{V_{cn}}{G_{12}^{cn}} + \frac{V_m}{G^{m}} \quad (5)$$

$$\nu = V_{cn}\nu^{cn} + V_m \nu^{m} \quad (6)$$

$$\rho = V_{cn}\rho^{cn} + V_m \rho^{m} \quad (7)$$

Wherein, $E_{11}^{cn}, E_{22}^{cn}, G_{12}^{cn}, \nu^{cn}$ are the modulus of elasticity, shear modulus, Poisson's ratio, and density of carbon nanotube, and E^{m}, G^{m}, ν^{m} و ρ^{m}, correspond to properties of the matrix. $\eta_j \ (j = 1,2,3)$ is the effectiveness coefficient of the carbon nanotube, which is derived from the compatibility of the answers achieved from the extended rule of mixture, and the answers achieved from the molecular dynamics method.

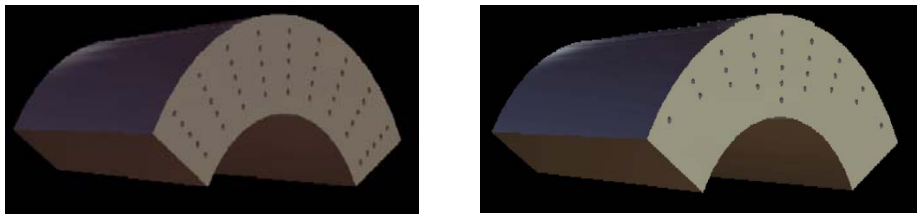

a: UD *b: FG –V*

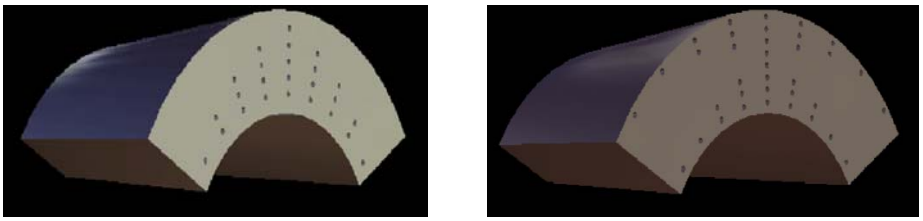

c: FG – Λ *d: FG-X*

Fig. 2.Distribution kind of carbon nanotube in the panel, a: Unidirectional (UD) form, b: V form, c: Λ form, and d: X form.

Governing motion equations

The governing three dimensional motion equations of the problem are as follows:

$$\frac{\partial \tau_{zr}}{\partial z}+\frac{1}{r}\frac{\partial \tau_{\theta r}}{\partial \theta}+\frac{\partial \sigma_r}{\partial r}+\frac{\sigma_r-\sigma_\theta}{r}=\rho\frac{\partial^2 u_r}{\partial t^2} \tag{8}$$

$$\frac{\partial \tau_{\theta z}}{\partial z}+\frac{\partial \sigma_\theta}{r\partial \theta}+\frac{\partial \tau_{r\theta}}{\partial r}+\frac{2\tau_{r\theta}}{r}=\rho\frac{\partial^2 u_\theta}{\partial t^2} \tag{9}$$

$$\frac{\partial \sigma_z}{\partial z}+\frac{\partial \tau_{z\theta}}{r\partial \theta}+\frac{\partial \tau_{rz}}{\partial r}+\frac{\tau_{rz}}{r}=\rho\frac{\partial^2 u_z}{\partial t^2} \tag{10}$$

The stress-displacement relations in the cylindrical coordinate system are defined as follows:

$$\varepsilon_r=\frac{\partial u_r}{\partial r} \qquad \varepsilon_\theta=\frac{u_r}{r}+\frac{\partial u_\theta}{r\partial \theta}$$

$$\gamma_{r\theta}=\frac{-u_\theta}{r}+\frac{\partial u_\theta}{\partial r}+\frac{\partial u_r}{r\partial \theta} \qquad \gamma_{zr}=\frac{\partial u_z}{\partial r}+\frac{\partial u_r}{\partial z}$$

$$\varepsilon_z=\frac{\partial u_z}{\partial z} \qquad \gamma_{z\theta}=\frac{\partial u_\theta}{\partial z}+\frac{\partial u_z}{r\partial \theta} \tag{11}$$

Where u_r, u_θ, and u_z are the radial, circumferential, and axial displacements, respectively. Boundary conditions for the panel are [23]:

$$r = a, b \qquad \sigma_r = \tau_{rz} = \tau_{r\theta} = 0 \tag{12}$$

$$\theta = 0, \Phi \qquad u_r = \sigma_\theta = \tau_{\theta z} = 0 \tag{13}$$

Semi Analytical Solution

The general relations for the displacement components, which satisfy the boundary conditions, are as follows:

$$\begin{aligned} u_r &= \sum_{m=1}^{\infty} \sin(\beta_m \theta).U_r(r).e^{i\omega t} \\ u_\theta &= \sum_{m=1}^{\infty} \cos(\beta_m \theta).U_\theta(r).e^{i\omega t} \\ u_z &= \sum_{m=1}^{\infty} \cos(\beta_m \theta).U_z(r).e^{i\omega t} \end{aligned} \tag{14}$$

$$\beta_m = \frac{m\pi}{\Phi} \ (m = 1, 2, ...) \tag{15}$$

Where, m is the number of the waves in the circumferential direction of the cylindrical panel. The differential quadrature method was first used by Bellman and Casti in 1971, as a numerical method to solve the partial differential equations [24]. In this method, if a grid of $N \times 1$ points of a physical area are considered in a way that N be the number of the grid points along the x axis, then the differential quadrature rules for the derivatives of a supposed function like $f(x)$ are stated as follows [25]:

$$\frac{\partial^n f(x_i)}{\partial x^n} = \sum_{k=1}^{N} c_{ik}^{(n)} f(x_k) \quad i = 1,..,N, \ n = 1,..,N-1 \tag{16}$$

Wherein, $c_{ik}^{(n)}$ is the weight coefficient related to the x-direction. According to the generalized quadrature method, the weight coefficients are calculated as follows [24]:

$$c_{ij}^{(1)} = \frac{M^{(1)}(x_i)}{(x_i - x_j) M^{(1)}(x_j)} \qquad i, j = 1,2,..,N, i \neq j \tag{17}$$

$$M^{(1)}(x_i) = \prod_{j=1, i \neq j}^{N} (x_i - x_j) \tag{18}$$

$$c_{ij}^{(n)} = n\left(c_{ii}^{(n-1)} c_{ij}^{(1)} - \frac{c_{ij}^{(n-1)}}{\left(x_i - x_j\right)} \right) \tag{19}$$

$$i, j = 1,2,\ldots N, i \neq j, n = 2,3,\ldots, N-1$$

$$c_{ii}^{(n)} = -\sum_{j=1, i\neq j}^{N} c_{ij}^{(n)} \quad i=1,2,\ldots N, n=1,2,\ldots,N-1 \tag{20}$$

The distribution kind of the grid points, which is generally used in papers, is in the normalized shape in the range of [0, 1], and is stated as follows [26]:

Sample points of Chebyshev-Gauss-Lobatto*)* (C-G-L)

$$x_i = \frac{1}{2}\left(1 - \cos\left(\frac{i-1}{N-1}\pi\right)\right) \qquad i = 1,2,\ldots,N \tag{21}$$

Now, in this stage, by applying the generalized differential quadrature method, equations (8) to (10) are made discrete. As a result, in each point of the r_i grid, with $i=2,\ldots, N$-1, the motion equation of (8) after becoming discrete is expressed as follows:

$$\begin{aligned}
&\sum_{k=1}^{N}((\bar{C}_{44})_i \frac{1}{r}\beta_m c_{ik}^{(1)} + (\bar{C}_{23})_i \frac{1}{r}\beta_m c_{ik}^{(1)})\ U_{\theta k} \\
&+\sum_{k=1}^{N}(((\frac{\partial \bar{C}_{33}}{\partial r})_i + (\bar{C}_{33})_i \frac{1}{r}) c_{ik}^{(1)} - ((\bar{C}_{45})_i + \\
&(\bar{C}_{36})_i)\frac{1}{r}\beta_m \sum_{k=1}^{N} c_{ik}^{(1)} U_{zk} + ((\bar{C}_{26})_i \frac{1}{r^2}\beta_m - \\
&(-(\frac{\partial \bar{C}_{23}}{\partial r})_i \frac{1}{r}\beta_m + ((\bar{C}_{22})_i + (\bar{C}_{44})_i)\frac{1}{r^2}\beta_m) U_{\theta i} + ((\frac{\partial \bar{C}_{23}}{\partial r})_i \\
&\frac{1}{r} - (\bar{C}_{22})_i \frac{1}{r^2} - (\bar{C}_{44})_i \frac{1}{r^2}\beta_m^2)\ U_{ri} + (\bar{C}_{33})_i c_{ik}^{(2)}) U_{rk} \\
&(\frac{\partial \bar{C}_{36}}{\partial r})_i \frac{1}{r}\beta_m) U_{zi} = -\omega^2 \rho U_{ri}
\end{aligned} \tag{22}$$

Where, $c_{ik}^{(1)}$ and $c_{ik}^{(2)}$ are first and second order weight coefficients, respectively.

Similarly, by applying the generalized differential quadrature method at the boundary conditions, the equations are made discrete as follows. Therefore, for the boundary conditions at $r=a$, we have:

$$\begin{aligned}
&(\bar{C}_{23})_1 \frac{1}{a} U_{r1} - (\bar{C}_{23})_1 \frac{1}{a} \beta_m U_{\theta 1} + \\
&(\bar{C}_{33})_1 \sum_{k=1}^{N} c_{1k}^{(1)} U_{rk} - (\bar{C}_{36})_1 \frac{1}{a}\beta_m U_{z1} = 0
\end{aligned} \tag{23}$$

$$-(\bar{C}_{44})_1 \frac{1}{a} U_{\theta 1} + (\bar{C}_{44})_1 \sum_{k=1}^{N} c_{1k}^{(1)} U_{\theta k} + (\bar{C}_{44})_1 \frac{1}{a} \beta_m U_{r1} + (\bar{C}_{45})_1 \sum_{k=1}^{N} c_{1k}^{(1)} U_{zk} = 0 \quad (24)$$

$$-(\bar{C}_{45})_1 \frac{1}{a} U_{\theta 1} + (\bar{C}_{45})_1 \sum_{k=1}^{N} c_{1k}^{(1)} U_{\theta k} + (\bar{C}_{45})_1 \frac{1}{a} \beta_m U_{r1} + (\bar{C}_{55})_1 \sum_{k=1}^{N} c_{1k}^{(1)} U_{zk} = 0 \quad (25)$$

Similarly, for the boundary conditions at the value of $r=b$ are achieved as above. The motion equations after getting discrete are rewritten in the matrix form as follows:

$$[A_{db}]\{U_b\} + [A_{dd}]\{U_d\} = -\rho\omega^2 \{U_d\} \quad (26)$$

Similarly, the boundary conditions can also be written as follows:

$$[A_{bb}]\{U_b\} + [A_{bd}]\{U_d\} = \{0\} \quad (27)$$

By substituting the relation (27) into relation (26), the eigenvalue problem is resulted with the following general form:

$$\left([A] + \rho\omega^2 [I]\right)\{U_d\} = \{0\} \quad (28)$$

Where:

$$[A] = [A_{dd}] - [A_{db}][A_{bb}]^{-1}[A_{bd}] \quad (29)$$

With this sequence, the system of the eigenvalue equations is achieved, and by using MATLAB software, the equation (28) is solved, and later the appropriate program for deriving the natural frequencies of the infinite functionally graded cylindrical panel reinforced by carbon nanotubes has been developed.

Verification

As it was stated in the previous section, the differential quadrature method is a numerical method; therefore the correctness of the results must be verified first. For verification purposes, the results of the present study have been compared with the results of the study performed by Sobhani *et al*. [21] on an orthotropic cylindrical panel, with an infinite length, for different angle values of the panel inlet *(Φ)*, and the index of power distribution of *p*, and the results achieved are presented in table (1). As it is perceived, there is a good compatibility between the results.

Table 1 .Comparison of the dimensionless frequency parameter $\Omega = \omega r_i \sqrt{\frac{\rho^{cu}}{E^{cu}}}$ *for the functionally graded orthotropic cylindrical panel, with an infinite length (v_{cu}= 0.28, ρ_w =19300 kg/m^3, E_w= 400 Gpa, v_{cu} = 0.31, ρ_{cu}= 8960 kg/m^3, E_{cu}= 115 Gpa, S=10, m=1).*

Φ	*P*=0	*P*=0.7	*P*=1	*P*=10	*P*=20
π/6					
a	1.1754	1.1025	1.0833	1.0805	1.0651
[21]	1.1572	1.0863	1.0485	1.0371	1.0049
π/3					
a	0.2719	0.2545	0.2427	0.2436	0.2397
[21]	0.2674	0.2421	0.2377	0.2353	0.2301
π/2					
a	0.969	0.0907	0.0890	0.0905	0.0880
[21]	0.0946	0.0866	0.0847	0.0840	0.0822

a: Present+ study.

Properties of the material

Properties of the carbon nanotube (10, 10) and its polymer are presented in table 2, according to reference [10]. The name of the polymer used is Methyl methacrylate, which is supposed to be isotropic. The dimensionless frequency parameter of Ω is defined with the $\Omega = \omega_{mn} 10h \sqrt{\frac{\rho^{cn}}{E_{11}^{cn}}}$ relation, where ρ^{cn}, E_{11}^{cn} are the density, and modulus of elasticity of the nanotube, respectively, and ω_{mn} is the natural frequency of the cylindrical panel.

Table 2 .Mechanical properties of the matrix and nanotube.

Mechanical Properties	*Matrix*	*Nanotube*
E_{11}	2.5 GPa	600 GPa
E_{22}	2.5 GPa	10 GPa
ρ	1150 kg/m^3	1400 kg/m^3
υ	0.34	0.19

Investigation of the convergence of the differential quadrature method

In figure (3)**,** convergence and accuracy of the base frequency parameter, according to the number of the sample points along the radius of the functionally graded panel reinforced by nanotubes, have been shown for different values of *S*. By increasing the number of points, the diagram becomes convergent, and also variations of the number of points will not have any effect on the accuracy of the answers. In figure (3), in order to show the accuracy and convergence of the semi-analytical method used, variations of the base frequency parameter of the functionally graded orthotropic panel reinforced by nanotubes have been presented for different values of *S*. It is necessary to

be stated that, in the solution based on the three dimensional elasticity equations, all the boundary conditions are simply supported.

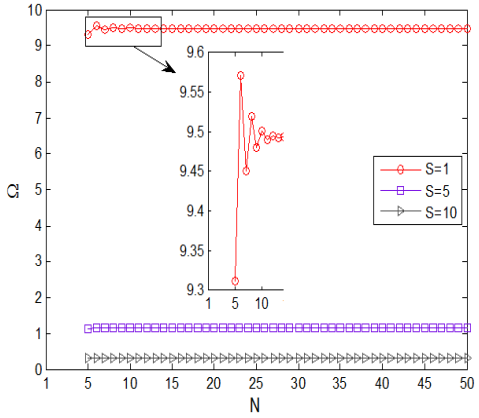

Fig. 3. Convergence and stability of the base frequency parameter of the FG panel reinforced by V form nanotubes for different values of S (m= 1, Φ= π/6).

Effectiveness coefficient of the carbon nanotube

Because of the van der Waals bond between carbon nanotube and polymer, transfer of load between the nanotube and the polymer phase does not fully take place, and since the rule of mixtures is only applicable to continuum environments, it is not possible to directly use this rule. Also, micromechanical relations like the rule of mixtures are not capable of considering the difference between the nano and micro scales; therefore Shen used the effectiveness coefficient $(\eta_j)$to overcome this problem for the carbon nanotubes [11, 12]. Values of η_j for different volume fractions of V_{CN}^{*} have been derived from the analogy of the modulus of elasticity between composites reinforced with carbon nanotubes, being achieved from the molecular dynamics simulation, using the predictions done by means of the expanded rule of mixtures. In table (3), different values of η_j have been presented for different values of V_{CN}^{*} . Shen considered this relation to exist between the effectiveness coefficients for carbon nanotubes: $\eta_3 = 0.7\eta_2$.

Table 3 .Comparison of the Young's modulus of nanocomposites reinforced by single walled carbon nanotubes (10, 10) at T_0=300 [11].

V_{cn}^{*}	*Molecular dynamics* [10]		*Extended rule of mixtures*			
	E_{11}(GPa)	E_{22}(GPa)	E_{11}(GPa)	η_1	E_{22}(GPa)	η_2
0.12	94.6	2.9	94.78	1.2833	2.9	1.0556
0.17	138.9	4.9	138.68	1.3414	4.9	1.7101
0.28	224.2	5.5	224.50	1.3238	5.5	1.7380

As it is seen, the values of the effectiveness coefficient stated in the above table, are achieved from the comparisons made between the studies performed on carbon nanotubes (10, 10) by Shen [11] and references [6, 10].

Investigation of the effect of different parameters on frequency parameter

In this section, the effects of the nominator of the transverse wave, *m*, on the frequency parameter are investigated. In figure (4a), variations of the frequency parameter versus the number of circumferential waves of the panel uniformly reinforced by carbon nanotubes, have been presented for different volume fractions of the nanotube. This figure shows that the increase of the number of transverse waves, and also the increase of the volume fraction of the nanotube, increases the base frequency parameter. It is necessary to be stated that, the number of the sample points is chosen to be N=17, and the volume fraction of the nanotube is supposed to be V_{cn}^{*}=0.28 in all the figures.

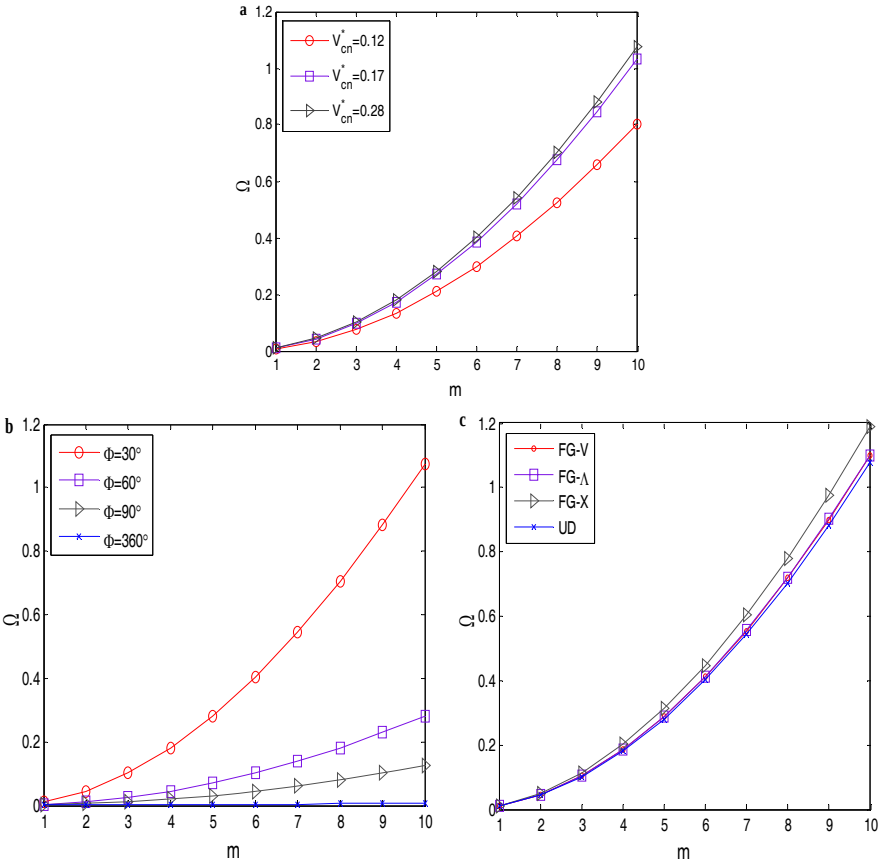

Fig. 4 .Variations of the frequency parameter versus the number of circumferential waves for: (a) different volume fractions of the nanotube, (b) different inlet angles of the panel, (c) different kinds of nanotube distribution in the panel (S= 100, Φ= π/6).

In figure (4b), variations of the frequency parameter versus number of circumferential waves have been shown for different inlet angles of the cylindrical panel, and it is seen that increase of the size of the inlet of the panel, decreases the frequency parameter, and also, the increase of the number of circumferential waves, increases the frequency parameter of the panel. Nanotube distribution in this figure is of uniform shape. In figure (4c), variations of the frequency parameter, versus number of circumferential waves have been shown for different kinds of the nanotube distribution in the cylindrical panel, and as it is was stated earlier, and as it is observed here in this figure, the highest value of the frequency parameter for the nanotube distribution exists for the *X* form.

In figure (5), the base frequency parameter of the panel reinforced by carbon nanotubes has been shown in terms of the number of transverse waves and different values of *S* parameter. Figure (5) indicates the fact that, necessarily by decreasing the radius to thickness ratio, *S*, and increasing the number of waves; the maximum value of the base frequency is not achieved. For better understanding of this issue, a three dimensional diagram of the frequency parameter has been presented, in terms of the number of the transverse waves, the radius to thickness ratio, *S*, for different inlet angles of the panel, and also for the uniform nanotube distribution.

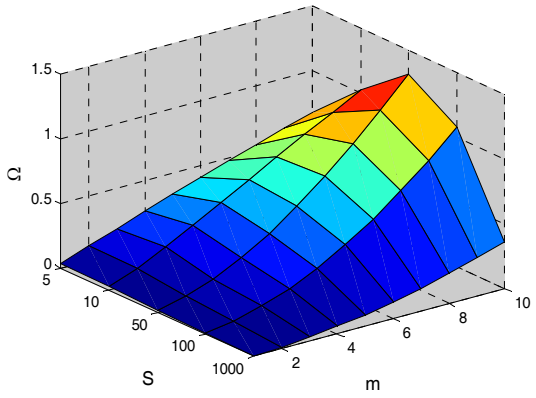

Fig. 5 .Variations of the frequency parameter in terms of circumferential waves (m) and parameter S (Φ= π/6).

Now, the effect of the middle radius to thickness ratio of the panel, *S*, on the base frequency parameter is investigated. In figure (6a), the effects of the middle radius to thickness ratio of the panel, *S*, on the dimensionless base frequency parameter of the FG cylindrical panel uniformly reinforced by carbon nanotubes has been shown for different volume fractions. By the increase of the volume fraction of the nanotube, for different values of the *S* ratio, the frequency parameter increases, and as the *S* ratio increases, the frequency parameter decreases. The effect of different kinds of nanotube distribution on the base frequency parameter of the FG orthotropic cylindrical panel with infinite length, in terms of the *S* parameter, has been shown in figure (6b). In this figure, it is shown that the kind of nanotube distribution in the FG cylindrical panel with infinite length, for the variations of the *S* ratio, has little effect on the frequency parameter. The effect of inlet angle of panel on the base frequency parameter of the FG

cylindrical panel reinforced by carbon nanotubes, in terms of the *S* parameter, has been presented in figure (6c). In this figure, nanotube distribution in the cylindrical panel is considered to be of *V* form. As it is seen, by the increase of the *S* ratio and the inlet angle of panel, the base frequency parameter is decreased.

Conclusion

In this paper, the vibration analysis of a FG polymeric cylindrical panel reinforced by carbon nanotubes has been investigated, based on the three dimensional elasticity theory, using the extended differential quadrature method.

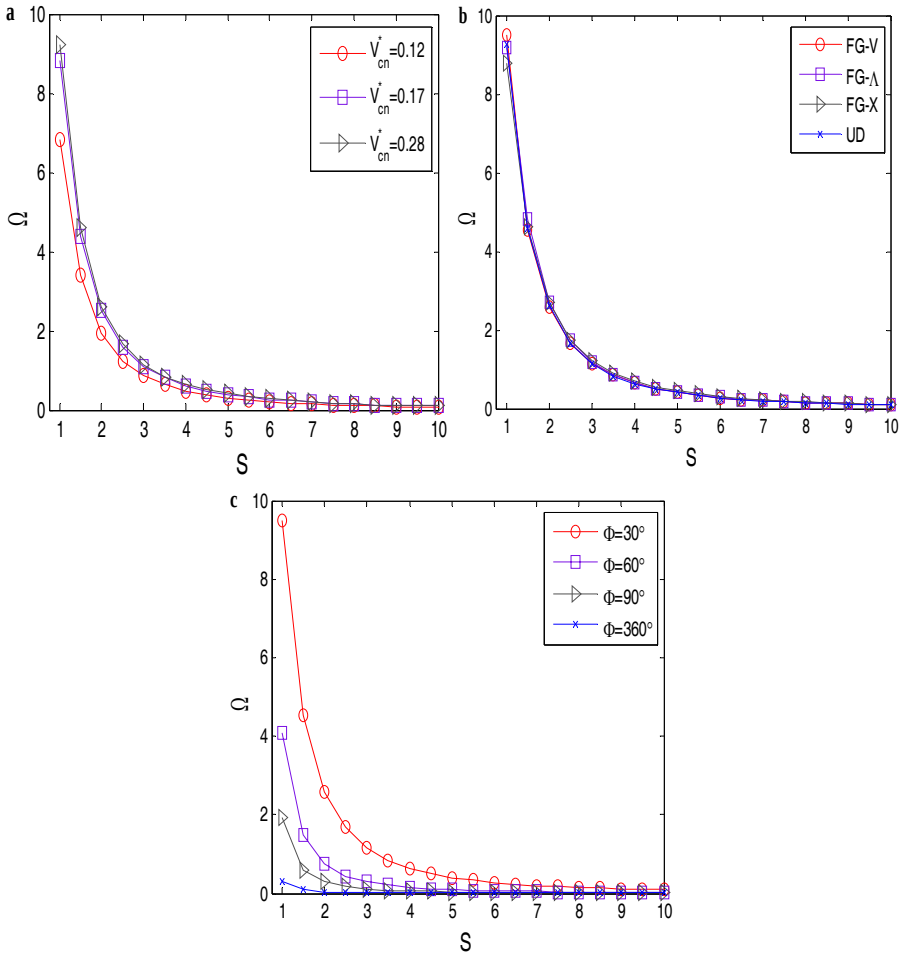

Fig. 6. Variations of the frequency parameter versus S for: (a) different volume fractions of nanotube, (b) different kinds of nanotube in the cylindrical panel, (c) different inlet angels of the panel.

Gradual change of material properties is considered as the linear volume fraction, at the constant volume percentage of the carbon nanotube. Since, so far no studies have

been performed on the vibrations of the FG cylindrical panel reinforced by carbon nanotubes, this study is aimed at understanding the vibration behavior of these new set of materials. In the current study, variations of the volume fraction of the carbon nanotube are considered along the radial direction, and the properties of the materials are achieved from the micromechanical model of the materials, but the micromechanical model of the materials is not capable of distinguishing the difference between nano and micro scales, therefore, in order to cope with this problem, an effectiveness coefficient of η is used. The effect of the volume fraction of the carbon nanotube, different boundary conditions, and also kinds of the nanotube distribution in the FG cylindrical panel reinforced by carbon nanotubes have been investigated in this article.

Reference

[1] H. Dai, 2002. Carbon nanotubes: opportunities and challenges, Surf. Sci. 500: 218-241.

[2] I. Kang, Y. Heung, J. Kim, J. Lee, R. Gollapudi, S. Subramaniam, S. Narasimhadevara, D. Hurd, G. Kirkera, V. Shanov, M. Schulz, D. Shi, J. Boerio, S. Mall, D. Ruggles-Wren, 2006. Introduction to carbon nanotube and nanofiber smart materials, Compos. Part B, 37: 382-394.

[3] K.T. Lau, C. Gu, D. Hui, 2006. A critical review on nanotube and nanotube/nanoclay related polymer composite materials, Compos. Part B, 37:425-436.

[4] Thostenson ET, Ren ZF, Chou TW, 2001. Advances in the science and technology of carbon nanotubes and their composites: a review. Compos Sci Technol, 61:1899-1912.

[5] Odegard GM, Gates TS, Wise KE, Park C, Siochi EJ, 2003. Constitutive modelling of nanotube-reinforced polymer composites, Compos Sci Technol, 63:1671-1687.

[6] M. Griebel, J. Hamaekers, 2004. Molecular dynamic simulations of the elastic moduli of polymer-carbon nanotube composites, Comput. Meth. Appl. Mech. Eng,193: 1773-1788.

[7] Cadek M, Coleman JN, Barron V, Hedicke K, Blau WJ, 2002. Morphological and mechanical properties of carbon-nanotube-reinforced semicrystalline and amorphous polymer composites. Appl Phys Lett; 81: 5123-5125.

[8] Thostenson ET, Chou TW, 2003. On the elastic properties of carbon nanotube-based composites. Modeling and characterization. J Phys-Appl Phys, 36: 573-582.

[9] J. D. Fidelus, E. Wiesel, F. H. Gojny, K. Schulte, H. D. Wagner, 2005. Thermo-mechanical properties of randomly oriented carbon/epoxy nanocomposites. Compos. Part A, 36: 1555-1561.

[10] Y. Han, J. Elliott, 2007. Molecular dynamics simulations of the elastic properties of polymer/carbon nanotube composites. Comput. Mater. Sci, 39: 315-323.

[11] H. S. Shen, 2009. Nonlinear bending of functionally graded carbon nanotube reinforced composite plates in thermal environments. Compos. Struct, 91: 9-19.

[12] H. S. Shen, 2011. Postbuckling of nanotube-reinforced composite cylindrical shells in thermal environments, Part I: Axially-loaded shells, Postbuckling of nanotube-reinforced composite cylindrical shells in thermal environments, Part I: Axially-loaded shells, Compos. Struct, 93: 2096-2108.

[13] B. Sobhani Aragh, M. H. Yas, 2010. Static and free vibration analyses of continuously graded fiber-reinforced cylindrical shells using generalized power-law distribution. Acta Mech, 215: 155-173.
[14] F. Tornabene, E. Viola, 2009. Free vibrations of four- parameter functionally graded parabolic panels and shells of revolution. European Journal of Mechanics A/Solids, 28: 991-1013.
[15] L. Li, R. Kettle, 2002. Nonlinear bending response and buckling of ring-stiffened cylindrical shells under pure bending. International Journal of Solids and Structures, 39: 765-781.
[16] A. Alibeigloo, V. Nouri, 2010. Static analysis of functionally graded cylindrical shell with piezoelectric layers using differential quadrature method. Composite Structures, 92: 1775-1785.
[17] D. Redekop, 2006. Three-dimensional free vibration analysis of inhomogeneous thick orthotropic shells of revolution using differential quadrature. Journal of Sound and Vibration, 291: 1029-1040.
[18] S.C. Pradhan, C.T. Loy, K.Y. Lam, J.N. Reddy, 2000. Vibration characteristics of functionally graded cylindrical shells under various boundary conditions. Applied Acoustics, 61: 111-129.
[19] F. Pellicano, 2003. Vibrations of circular cylindrical shells: Theory and experiments. Journal of Sound and Vibration, 303:154-170.
[20] W. Jiang, D. Redekop, 2003. Static and vibration analysis of orthotropic toroidal shells of variable thickness by differential quadrature. Thin-Walled Structures, 41: 461-478.
[21] B. Sobhani Aragh, M. H. Yas, 2010. Three-dimensional free vibration of functionally graded fiber orientation and volume fraction cylindrical panels. Mater. Design, 31, 4543-4552.
[22] J. N. Reddy, 2004. Mechanics of laminated composite plates and shells. New York, CRC Press.
[23] A. Alibeigloo and M. Shakeri, 2005. Dynamic Analysis of Orthotropic Laminated Cylindrical Panels. Mechanics of Advanced Materials and Structures, 12: 67-75.
[24] R. E. Bellman and J. Casti, 1971. Differential quadrature and long-term integration. Mathematical Analysis Application, 34: 235-238.
[25] C. Shu and B. E. Richards, 1992. Application of generalized differential quadrature to solve two-dimensional incompressible Navier-Stokes equations. Numerical Methods Fluids, 15: 791-798.
[26] F. Tornabene and E.Viola, 2008. 2D solution for free vibration of parabolic shells using generalized differential quadrature method. European Journal of Mechanics A/solids, 27 (6): 1001-1025.